Hindawi
Advances in Polymer Technology
Volume 2019, Article ID 2369329, 8 pages
https://doi.org/10.1155/2019/2369329

Research Article

Pseudo-Elastic Analysis with Permanent Set in Carbon-Filled Rubber

LiHong Huang[1,2] **Xiaoxiang Yang**[1,3] **and Jianhong Gao**[1,3]

[1]*College of Chemical Engineering, Fuzhou University, Fuzhou, Fujian 350108, China*
[2]*Fuzhou University Zhicheng College, Fuzhou, Fujian 350002, China*
[3]*Quanzhou Normal University, Quanzhou, Fujian 362000, China*

Correspondence should be addressed to Xiaoxiang Yang; yangxx@fzu.edu.cn

Received 15 September 2018; Revised 5 November 2018; Accepted 8 November 2018; Published 3 January 2019

Academic Editor: Siu N. Leung

Via cyclic loading and unloading tests of natural/styrene-butadiene rubber (NSBR) blends at room temperature, the effects of the stretching, rate, temperature, and volume fraction of carbon black in the filled rubber on a permanent set (residual strain) were studied. The results showed that increasing the stretching, rate, and volume fraction of carbon black and reducing the temperature yielded greater residual strain. The uniaxial tensile behaviors of composites with the Mullins effect and residual strain were simulated using the ABAQUS software according to the aforementioned data. An Ogden-type constitutive model was derived, and the theory of pseudo-elasticity proposed by Ogden and Roxburgh was used in the model. It was found that the theory of pseudo-elasticity and the Ogden constitutive model are applicable to this composite, and if combined with plastic deformation, the models are more accurate for calculating the residual strain after unloading.

1. Introduction

Carbon black-filled rubber on the virgin loading shows significant hysteresis during the load–unload–reload–unload cycle, which is called the Mullins effect. The Mullins effect mainly depends on the proportion of filler in the rubber composites [1]. The Mullins effect is negligible in unfilled rubber but becomes obvious in rubber filled with a high carbon black content. The difference in stress during the first loading and unloading paths of a virgin carbon black-filled rubber specimen is greater than for any other loading and unloading cycle. The hysteresis area enclosed by the stress–strain curve between loading and unloading represents the dissipated energy. If some cycles with a constant stretch amplitude are conducted, the hysteresis area stabilizes. With some loading cycles, the stress heals after a certain amount of recovery time. The energy dissipation of rubber after a recovery is less than that of virgin rubber, but each subsequent stretching is always less severe than the previous stretching [2].

A theoretical model for the hyperelastic behavior of filled rubbers was proposed by Mullins and Tobin (1957) [3] and Mullins (1969) [4]. Ogden and Roxburgh (1999) [5, 6] used a single softening damage variable to model the idealized Mullins effect in filled rubber, which experiences not only uniaxial tension but also biaxial and multiaxial tension, while ignoring the residual strain. In 2001, Ogden calculated the stress softening and residual strain during the azimuthal shearing of a pseudo-elastic circular cylindrical tube [7]. Dorfmann and Ogden (2004) [8] proposed a constitutive model for the Mullins effect with a permanent set employing two damage variables in the energy-dissipation function. Related studies have been performed [9, 10], and different damage variables have been proposed [11–14]. In addition, the Mullins effect has been studied from a molecular viewpoint [15–17], and discussions on the Mullins effect have continued.

In this study, uniaxial tensile experiments involving different stretching ratios of natural/styrene-butadiene blends with different carbon black contents were performed, and the influences of different factors on the residual strain were investigated according to these experiments. A combination of the Mullins effect and plastic deformation theory was introduced using the Ogden–Roxburgh pseudo-elastic model, and the Mullins effect with the residual strain of the

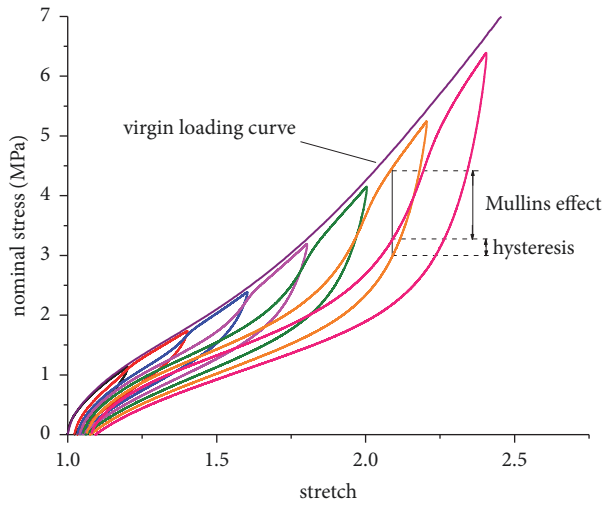

Figure 1: Mullins effect.

blends was simulated and verified using the finite-element software ABAQUS.

2. Mullins Effect

The cyclic stress–strain curves with different stretching amplitudes, as well as the virgin loading curve, for virgin rubber are presented in Figure 1. For loading and unloading cycles, the specimen was first loaded to a particular point and then unloaded, and the unloading curve was significantly lower than the loading curve. The second loading curve was lower than the virgin loading curve but higher than the first unloading curve prior to the virgin loading strain and recovered with a bigger strain. It was not fully restored to its original state when unloaded to zero stress, and residual strain (permanent set) was produced. The Ogden–Roxburgh pseudo-elasticity model and plastic deformation theory are used to describe the Mullins effect and residual strain.

3. Ogden–Roxburgh Pseudo-Elasticity Model

3.1. Ogden Constitutive Model. The Ogden (N = 3) (1972, 1982) [18] constitutive equation of the strain energy function for in-compressible stress-softening materials is as follows:

$$W_{Ogden} = \sum_{i=1}^{3} \frac{2\mu_i}{\alpha_i^2} \left(\lambda_1^{\alpha_i} + \lambda_2^{\alpha_i} + \lambda_3^{\alpha_i} - 3\right) \tag{1}$$

The uniaxial extension of a stretch is described as follows:

$$\begin{aligned} \lambda_1 &= \lambda, \\ \lambda_2 &= \lambda_3 = \lambda^{-1/2} \end{aligned} \tag{2}$$

The Ogden (N = 3) strain energy function under uniaxial tensile stress is given as follows:

$$W_{Ogden} = \sum_{i=1}^{3} \frac{2\mu_i}{\alpha_i^2} \left(\lambda^{\alpha_i} + 2\lambda^{-\alpha_i/2} - 3\right) \tag{3}$$

3.2. Ogden–Roxburgh Pseudo-Elasticity Model. The axial components of the Cauchy stress tensor for an incompressible isotropic material such as carbon-reinforced rubber are as follows:

$$\begin{aligned} \sigma_1 &= \sigma, \\ \sigma_2 &= \sigma_3 = 0 \end{aligned} \tag{4}$$

The material is continuously damaged during the loading and unloading paths, assuming that the damage function [5] defined as $\phi(\eta)$ indicates the energy dissipated during the loading and unloading paths. The damage variable was defined as η, which is given by (5). In the loading path, we set $\eta = 1$ and, in the unloading path, η was decreased within the range of $0 < \eta \leq 1$. The strain energy function was defined as $W(\lambda_1, \lambda_2, \eta)$, and we denote $W_0(\lambda, \lambda^{-1/2})$ in the loading path and $W(\lambda, \lambda^{-1/2}, \eta)$ in the unloading path, as described by (6). The Cauchy stress is described by (7), and the nominal stress is given by (8). The damage function and damage variable are described by (9) and (10), respectively.

$$\eta = \chi\left(\lambda, \lambda^{-1/2}\right) = \chi\left(\lambda^{-1/2}, \lambda\right) \tag{5}$$

$$W\left(\lambda, \lambda^{-1/2}, \eta\right) = \eta W_0\left(\lambda, \lambda^{-1/2}\right) + \phi\left(\eta\right), \quad 0 < \eta \leq 1 \tag{6}$$

$$\sigma = \lambda \frac{\partial W\left(\lambda, \lambda^{-1/2}, \eta\right)}{\partial \lambda} = \lambda\eta \frac{\partial W_0}{\partial \lambda} \tag{7}$$

$$t = \eta \frac{\partial W_0\left(\lambda, \lambda^{-1/2}\right)}{\partial \lambda} = \eta t_0 \tag{8}$$

$$-\phi'\left(\eta\right) = m\mathrm{Erf}^{-1}\left(r\left(\eta - 1\right)\right) + W_m \tag{9}$$

$$\eta = 1 - \frac{1}{r}\mathrm{Erf}\left[\frac{1}{m}\left(W_m - W_0\left(\lambda, \lambda^{-1/2}\right)\right)\right] \tag{10}$$

Here, Erf is the Gaussian error function, and $\mathrm{Erf}(x) = (2/\sqrt{\pi}) \int_0^x e^{-\eta^2} d\eta$.

3.3. Elasticity–Plasticity Theory. With the development of continuum elastoplastic theory, Lee [19] presented new concepts that must be introduced in order to formulate a satisfactory elastic–plastic theory when both the elastic and the plastic components of the strain can be finite, and the function is as follows:

$$F = F^e F^p \tag{11}$$

Here, F is the multiplicative decomposition of the deformation gradient, F^e is the elastic portion, and F^p is the plastic portion.

There is substantial discussion regarding elastoplastic separation, and it has been investigated by many scholars [20, 21]. It appears that a permanent set is generated by the plastic portion, and we can use the nonlinear elasticity model combined with plasticity and the Mullins effect to present the Mullins effect with the permanent set of rubber.

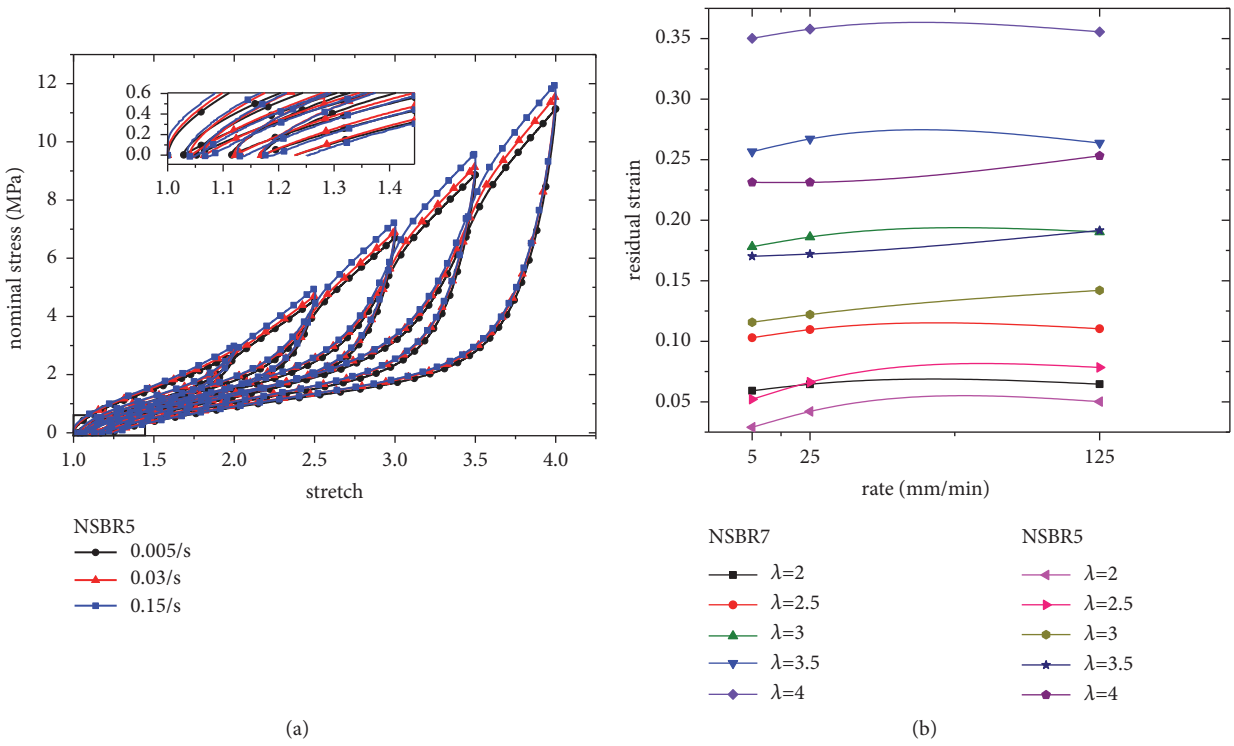

FIGURE 2: Curves of the residual strain and rate for the rubber: (a) the experimental results of NSBR5 for the Mullins effect at different rates of 0.005/s, 0.03/s, and 0.15/s and (b) the residual strain and rate of NSBR5 and NSBR7.

4. Experiments

4.1. Uniaxial Tensile Experiments. The prepared specimens satisfied the shape and size for dumbbell specimens of the National Standard, GB/T528-2009. Carbon black-filled natural/styrene-butadiene rubber (NSBR) blends were prepared using the same technological process and vulcanization. The ingredients of the carbon black-filled NSBR blends are shown in Table 1, including three kinds of rubber filled with different volumes of carbon black. The experiment was performed using an AG-Xplus 50KN Shimadzu material tester.

Uniaxial tensile loading–unloading–reloading–unloading experiments with different elongation ratios were performed at room temperature using a Shimadzu AG-plus 50 kN automatic control-testing machine. The residual strains during the experiments with different strain rates, stretching ratios, and carbon black volumes were examined.

4.2. Residual Strain. The carbon black-filled rubber samples were restored after a uniaxial tensile stress for a certain period of time. As a result, there remains a certain degree of residual strain that cannot be neglected. The residual strain is related to the stretching ratio, carbon black volume fraction, loading rate, and temperature, among other aspects. Figures 2–4 show the relationship between different factors and residual strain under the same conditions.

The relationships between the residual strain and the strain rate of the uniaxial loading–unloading cycle in the experimental curve of NSBR5 at different strain rates of 0.005/s, 0.03/s, and 0.15/s at room temperature are shown Figure 2. During the loading process, the rubber molecular chains and carbon black developed a slip deformation, and the stress increased with the increase of the strain rate because there was insufficient time to complete the slip, and the elastic modulus of the material increased. The hysteresis was related to the tensile rate during the loading–unloading–reloading–unloading process. When the tensile rate was higher, the residual strain became larger, and the modulus of the material was greater; however, this was not obvious at a low tensile rate.

Figure 3 shows the experimental curve for a rubber composite with carbon black volume fractions of 8.37%, 15.45%, and 20.08% at different stretching ratios of the uniaxial loading–unloading cycle, as well as the relationship between the residual strain and carbon black volume fractions at a tensile rate of 0.005/s at room temperature. As shown in Figure 3(b), the residual strain after unloading increased with the carbon black amount. With the addition of carbon black, the material was hardened, the modulus increased and rigid chains were formed between the carbon black and the rubber molecular chain. In addition, the residual strain increased with the increase of the stretching ratio for the same carbon content, but it increased slowly with a higher carbon black content.

Uniaxial tensile test curves obtained at different temperatures and the relationship between the residual strain and the temperature of carbon black-filled composites are shown in Figure 4. The uniaxial tensile stretching was 2 under a tensile rate of 0.005/s at temperatures of -40, -30, -15, 25,

Table 1: Ingredients of carbon black-filled NSBR composites.

Rubber	NR	SBR	N220	ZnO	Octadecanoic acid	Age resister 4020	Brimstone	Accelerant	Carbon black volume fraction
NSBR3	80	20	20	5	2	0.7	2.6	1.3	8.37%
NSBR5	80	20	40	5	2	0.7	2.6	1.3	15.45%
NSBR7	80	20	55	5	2	0.7	2.6	1.3	20.08%

Note. The data in the table indicate the quality of the components, in addition to the carbon black content.

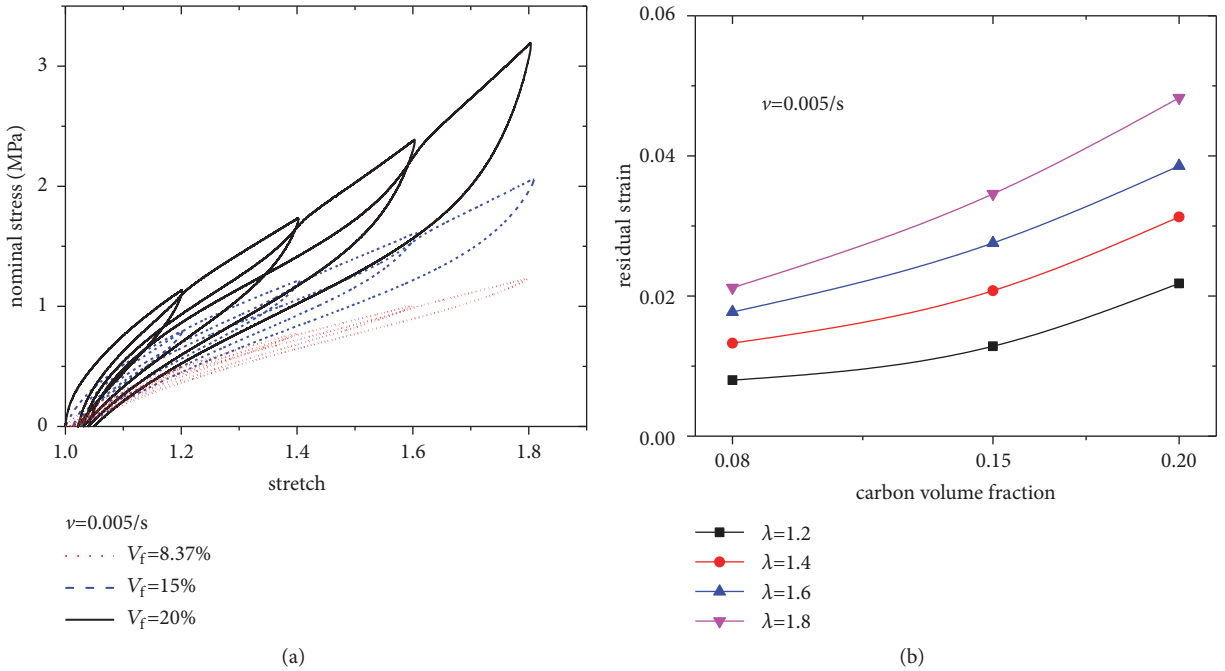

Figure 3: Curves of the residual strain and carbon volume fraction for the rubber: (a) experimental results of NSBR for the Mullins effect at a rate of 0.005/s and (b) the residual strain and carbon volume fraction.

40, 55, and 70°C. The rubber composites had different vitrification temperatures. As shown in Figure 4(a), in the low-temperature region of -40 to −15°C, the loading curve tended to be linear, indicating that it was close to its vitrification temperature. When the temperature was decreased from room temperature, the forces of the rigid chains between the rubber molecular chains and the carbon black were increased, the movement of rubber molecules was reduced, and the material was hardened; thus, the elastic modulus was increased. Therefore, the residual strain after unloading was larger at a lower temperature. However, when returning to room temperature, the flexible chains were restored, and the residual strain was dramatically decreased.

The mechanical properties were different when the temperature was above room temperature. In the range of 25–70°C, with the increase of the temperature, the composite material became softer, and the elastic modulus decreased, although the change was very slight. As shown in Figures 4(b) and 4(d), the residual strain of the two kinds of rubbers decreased with the increase of the temperature, but the change was significantly smaller than that in a low-temperature environment.

5. Simulation

5.1. Ogden–Roxburgh Pseudo-Elastic Model. Since Ogden and Roxburgh (1999) first proposed the pseudo-elasticity theory model, research on the Mullins effect of carbon black-filled rubber composites has continued, and it now involves the development of constitutive models. The Mooney–Rivlin constitutive model has good accuracy when the strain is small ($\varepsilon < 1.5$), although the Ogden constitutive model ($N = 3$) remains more accurate within a larger range. The Ogden constitutive model or the Marlow model [22] is usually chosen in studies, and the main problem has been that the pseudo-elastic model parameters r and m are not sufficiently accurate when other constitutive models are used. Therefore, the applicability and precision of the Ogden ($N = 3$) constitutive model are discussed for $\lambda < 2$.

Bi-square robust control and the Levenberg–Marquardt nonlinear least-squares method were used to fit the parameters using the MATLAB software. The parameters of the model were fitted to the experimental data from the loading and unloading tests with different stretching amplitudes of the NSBR blends at room temperature, as shown in

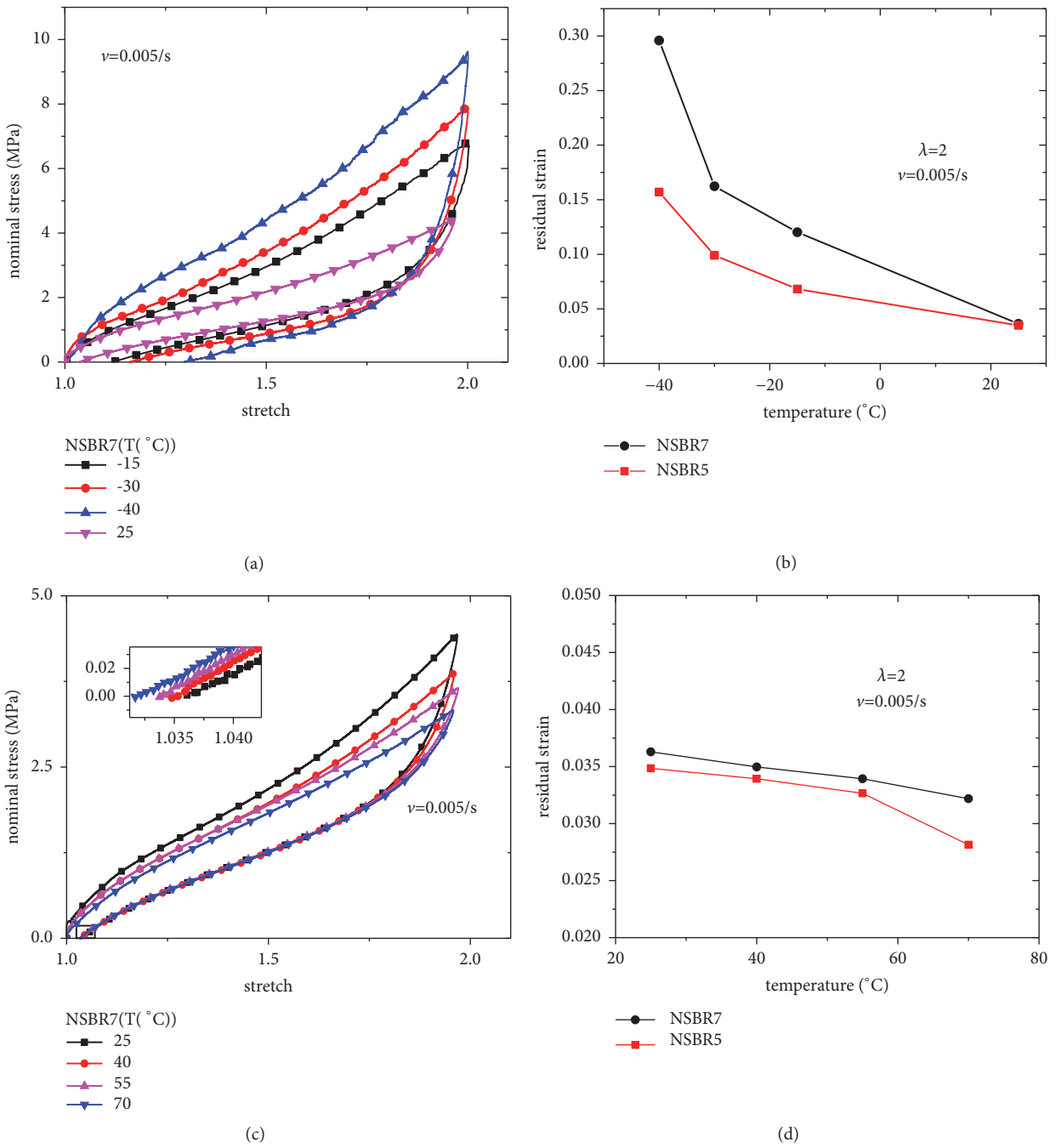

Figure 4: Curves of the residual strain and temperature of the rubber: (a) experimental results of NSBR7 for the Mullins effect at a rate of 0.005/s in the temperature range of -40–25˚C; (b) the residual strain vs. the temperature of NSBR5 and NSBR7 in the temperature range of -40–25˚C; (c) experimental results of NSBR7 for the Mullins effect at a rate of 0.005/s in the temperature range of 25–70˚C; (d) the residual strain and temperature of NSBR5 and NSBR7 in the temperature range of 25–70˚C.

Figure 3(a). The tensile rate was 0.005/s, and the stretching ratio was λ = 1.2, 1.4, 1.6, and 1.8. The results are shown in Table 2.

The hyperelastic behavior and Mullins effect were defined in the model. The Ogden–Roxburgh Pseudo-elastic model was used to simulate the uniaxial loading–unloading cycle of carbon black-filled rubber at different stretching ratios. Experimental and simulation curves obtained without considering the residual strain of NSBR5 and NSBR7 are shown in Figures 5 and 6, respectively, and the stretching ratio is λ = 1.2, 1.4, 1.6, and 1.8 with a tensile rate of 0.005/s.

As shown in the figures, the simulation curves for the two kinds of materials are basically in agreement with the experimental curves, and their root-mean-square error (*RSME*)

Table 2: Summary of the model parameters for virgin loading curves of NSBR5 and NSBR7.

rubber	parameter							
	Ogden constitutive model						pseudo-elasticity model	
	μ_1/MPa	α_1	μ_2/MPa	α_2	μ_3/MPa	α_3	r	m/MPa
NSBR5	-1.435	1.357	0.04542	4.551	3.884	-5.169	2.342	0.6172
NSBR7	-2.344	1.3	6.361	-6.112	-0.2074	4.604	1.812	1.066

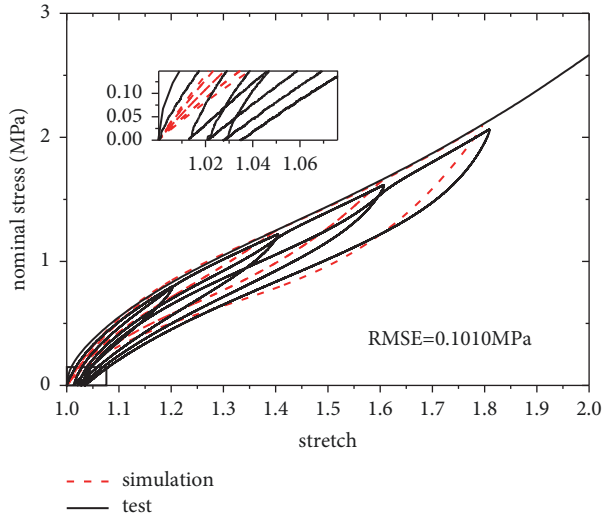

Figure 5: Experimental and simulation results of NSBR5 for the Mullins effect without the permanent set.

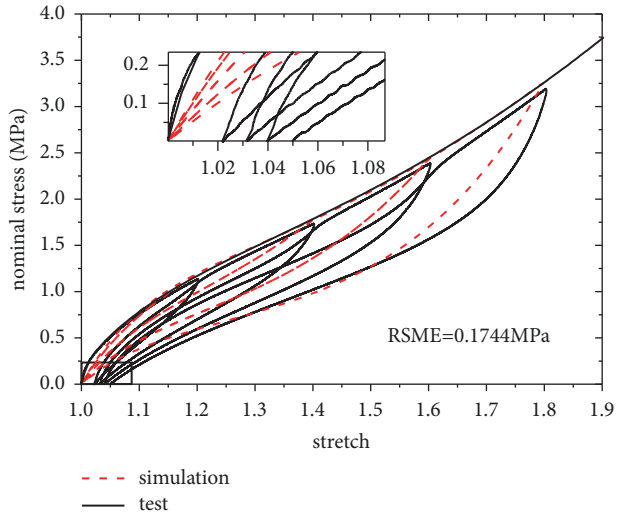

Figure 6: Experimental and simulation results of NSBR7 for the Mullins effect without the permanent set.

values are 0.1011 and 0.1744 MPa for NSBR5 and NSBR7, respectively. As reasons for these *RSME* values, the deviations of the simulation and experimental unloading curves within the small strain range ($\varepsilon < 0.5$) were greater than that of any other loading and unloading cycles, which indicates that the pseudo-elastic model is insufficiently accurate within a small strain range. In addition, the hysteresis effect causes the reloading curves to not exactly coincide with the unloading curves. However, the hysteresis and Mullins effects cannot be considered together in the ABAQUS software; thus, the error is unavoidable. The simulation and experimental unloading curves were different where the stress was close to zero, which indicates that the simulation curves are not effective for expressing the residual strain in an elastic material with continuous loading.

5.2. Ogden–Roxburgh Pseudo-Elastic Model with Plastic Deformation. Different residual strains are shown in the experimental curves of Figure 3 after unloading, and to reduce the deviation between the simulation and experimental results, the hyperelastic behavior and Mullins effect were defined in the model through a combination with the plastic deformation theory in the ABAQUS software. The given isotropic hardening function represents the degree of plastic deformation. The true stress and true strain curves of NSBR5 and NSBR7 correspond to the nominal stress and nominal strain curves shown in Figure 3(a). The residual strain is the plastic strain that can be gained from the plasticity data of different stretching ratios, i.e., $\lambda = 1.2$, 1.4, 1.6, and 1.8, as well as the true stress and elastic strain. The true stress–strain curve for NSBR5 is shown in Figure 7, for which the plasticity data were obtained from the results shown in Table 3.

According to the simulation results shown in Figures 5 and 6, the plastic deformation theory was combined to simulate the uniaxial loading–unloading cycle of carbon black-filled composites at different stretching ratios. Experimental and simulation curves for the NSBR5 and NSBR7 materials with a tensile rate of 0.005/s are shown in Figures 8 and 9, respectively, where the stretching ratio is 1.2, 1.4, 1.6, and 1.8. The *RSME* values of the nominal stress between the simulation and the experimental curves are 0.0909 and 0.1496 MPa for the NSBR5 and NSBR7 materials, respectively, which are smaller than those in Figures 5 and 6. At the initial position, the simulation curves showed the residual strain well. However, the reloading and unloading curves did not coincide, owing to the hysteresis. If the simulation and experimental unloading curves are consistent, a deviation between the simulation unloading curves and the experimental reloading curves is bound to exist because of the hysteresis. Even if the pseudo-elastic parameters of each cycle are calculated and substituted into the model separately, the unloading simulation curves of each cycle will be closer to the experimental unloading curves [23] but will increase their deviation with the experimental reloading curves. Therefore, a deviation is definitely unavoidable if the hysteresis cannot be considered in the model.

Table 3: Plasticity data obtained from the Mullins effect tests for NSBR5 and NSBR7.

Rubber	True stress σ_i	True strain ε_i	Plastic strain ε_{pi}	Elastic strain ε_{ei}
NSBR5	0.94922	0.18234	0.01275	0.16959
	1.69335	0.33652	0.02055	0.31597
	2.57041	0.47113	0.02737	0.44377
	3.70063	0.58975	0.03442	0.55533
NSBR7	1.35261	0.18366	0.02118	0.16249
	2.41748	0.33797	0.03009	0.30788
	3.78567	0.47192	0.03852	0.43340
	5.75115	0.58913	0.04801	0.54112

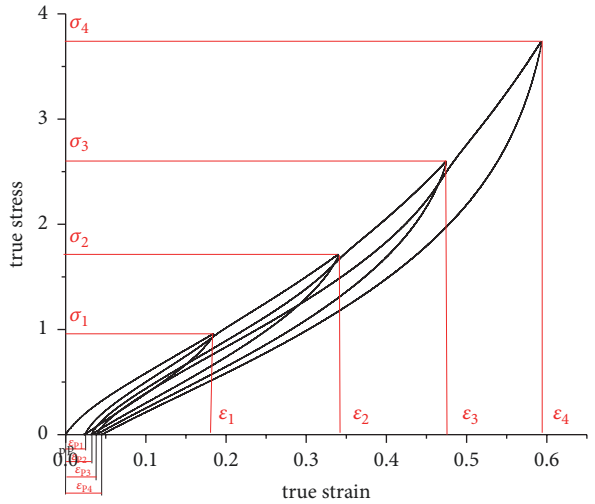

Figure 7: True stress–strain curve for the Mullins effect tests of NSBR5.

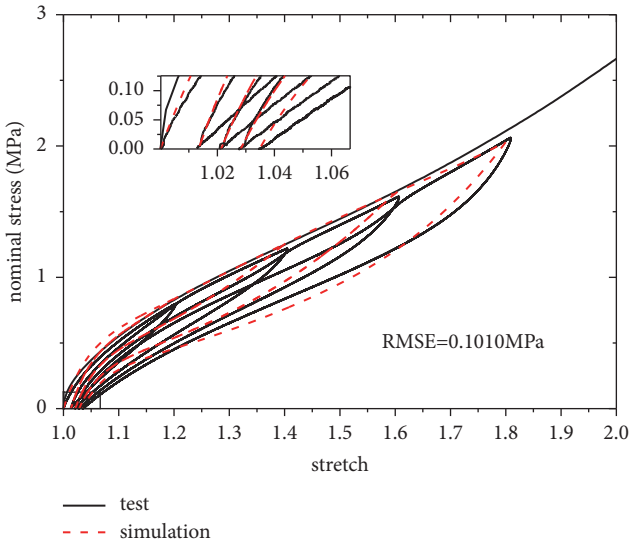

Figure 8: Experimental and simulation results of NSBR5 for the Mullins effect with the permanent set.

Thus, it was shown that the pseudo-elastic model with plastic deformation can be used to determine the residual strain well, with a low RSME and high precision. This is a good model for studying the Mullins cycle process of hyperelastic materials under stress softening and residual strain (permanent set).

6. Conclusion

The residual strain was shown to be greater when the tensile stretching ratio is higher, the carbon black content is higher, or the tensile rate is higher and the temperature (within the range of -40–70°C) is lower. According to a comparison of the experimental nominal stress–strain curves of the uniaxial tensile loading–unloading cycle of carbon black-filled rubber composites with no loading history and simulation results obtained using ABAQUS software, the Ogden–Roxburgh model can describe the hyperelasticity and Mullins effect well without residual strain. We can obtain better results by combining the Ogden–Roxburgh model with plastic deformation, which allows the residual strain to be calculated with high accuracy.

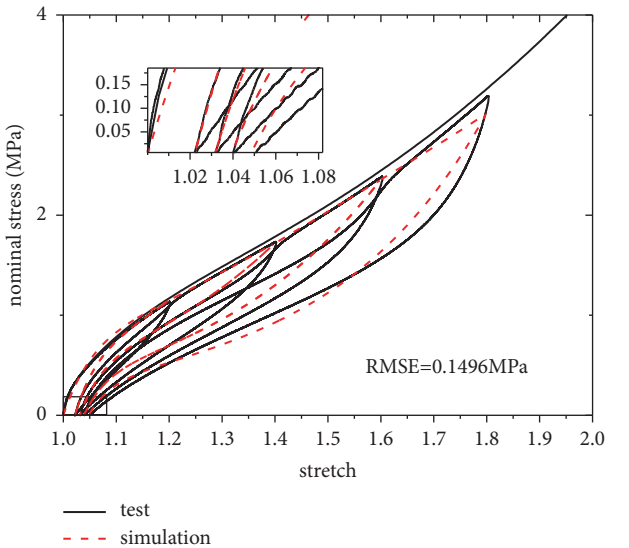

Figure 9: Experimental and simulation results of NSBR7 for the Mullins effect with the permanent set.

Data Availability

The data used to support the findings of this study are available from the corresponding author upon request.

Conflicts of Interest

The authors declare that they have no conflicts of interest.

Acknowledgments

This work was supported by the National Natural Science Foundation Project of China (Grant no. 11372074) and the Education Research Project for Young Teachers of Fujian Province (JAT170850), as well as the Natural Science Foundation of Fujian Province (no. 2018J01663) and 2016 Open Projects of the Key Laboratory for Strength and Vibration of Mechanical Structures (no. SV2016-KF-18).

References

[1] L. Mullins, "Effect of Stretching on the Properties of Rubber," *Rubber Chemistry and Technology*, vol. 21, no. 2, pp. 281–300, 1948.

[2] A. Lion, "A constitutive model for carbon black filled rubber: Experimental investigations and mathematical representation," *Continuum Mechanics and Thermodynamics*, vol. 8, no. 3, pp. 153–169, 1996.

[3] L. Mullins and N. R. Tobin, "Theoretical model for the elastic behaviour of filled-reinforced vulcanized rubbers," in *Rubber Chemistry and Technology*, vol. 37, pp. 551–557, 1957.

[4] L. Mullins, "Softening of Rubber by Deformation," *Rubber Chemistry and Technology*, vol. 42, no. 1, pp. 339–362, 1969.

[5] R. W. Ogden and D. G. Roxburgh, "A pseudo-elastic model for the Mullins effect in filled rubber," *Proceedings of the Royal Society A Mathematical, Physical and Engineering Sciences*, vol. 455, no. 1988, pp. 2861–2877, 1999.

[6] R. W. Ogden, "Elastic deformation of rubberlike solids," *Mechanics of solids*, pp. 499–537, 1982.

[7] R. W. Ogden, "Stress softening and residual strain in the azimuthal shear of a pseudo-elastic circular cylindrical tube," *International Journal of Non-Linear Mechanics*, vol. 36, no. 3, pp. 477–487, 2001.

[8] A. Dorfmann and R. W. Ogden, "A constitutive model for the Mullins effect with permanent set in particle-reinforced rubber," *International Journal of Solids and Structures*, vol. 41, no. 7, pp. 1855–1878, 2004.

[9] G. Palmieri, M. Sasso, G. Chiappini, and D. Amodio, "Mullins effect characterization of elastomers by multi-axial cyclic tests and optical experimental methods," *Mechanics of Materials*, vol. 41, no. 9, pp. 1059–1067, 2009.

[10] A. B. Chai, E. Verron, A. Andriyana, and M. R. Johan, "Mullins effect in swollen rubber: Experimental investigation and constitutive modelling," *Polymer Testing*, vol. 32, no. 4, pp. 748–759, 2013.

[11] S. R. Rickaby and N. H. Scott, "Cyclic stress-softening model for the Mullins effect in compression," *International Journal of Non-Linear Mechanics*, vol. 49, pp. 152–158, 2013.

[12] B. Meissner and L. Matějka, "A structure-based constitutive equation for filler-reinforced rubber-like networks and for the description of the Mullins effect," *Polymer Journal*, vol. 47, no. 23, pp. 7997–8012, 2006.

[13] A. Andriyana, M. S. Loo, G. Chagnon, E. Verron, and S. Y. Ch'Ng, "Modeling the Mullins effect in elastomers swollen by palm biodiesel," *International Journal of Engineering Science*, vol. 95, pp. 1–22, 2015.

[14] Y. Merckel, J. Diani, M. Brieu, and J. Caillard, "Constitutive modeling of the anisotropic behavior of Mullins softened filled rubbers," *Mechanics of Materials*, vol. 57, pp. 30–41, 2013.

[15] C. Ma, T. Ji, C. G. Robertson, R. Rajeshbabu, J. Zhu, and Y. Dong, "Molecular insight into the Mullins effect: Irreversible disentanglement of polymer chains revealed by molecular dynamics simulations," *Physical Chemistry Chemical Physics*, vol. 19, no. 29, pp. 19468–19477, 2017.

[16] G. Machado, G. Chagnon, and D. Favier, "Theory and identification of a constitutive model of induced anisotropy by the Mullins effect," *Journal of the Mechanics and Physics of Solids*, vol. 63, pp. 29–39, 2014.

[17] H. Khajehsaeid, "Development of a network alteration theory for the Mullins-softening of filled elastomers based on the morphology of filler-chain interactions," *International Journal of Solids and Structures*, vol. 80, pp. 158–167, 2016.

[18] R. W. Ogden, "Large deformation isotropic elasticity: on the correlation of theory and experiment for incompressible rubberlike solids," *Proceedings of the Royal Society of London A: Mathematical A*, vol. 326, no. 1567, pp. 565–584, 1972.

[19] E. H. Lee and D. T. Liu, "Finite-strain elastic—plastic theory with application to plane-wave analysis," *Journal of Applied Physics*, vol. 38, no. 1, pp. 19–27, 1967.

[20] K. C. Le and H. Stumpf, "Constitutive equations for elastoplastic bodies at finite strain: thermodynamic implementation," *Acta Mechanica*, vol. 100, no. 3-4, pp. 155–170, 1993.

[21] H. Stumpf and B. Schieck, "Theory and analysis of shells undergoing finite elastic-plastic strains and rotations," *Acta Mechanica*, vol. 106, no. 1-2, pp. 1–21, 1994.

[22] L. FanZhu, L. Jinpeng, and L. Longlai, "Modeling on constitutive behaviors of filled rubber compounds for cyclic loading path," *Rubber Chemistry and Technology*, vol. 64, no. 2, pp. 79–83, 2017.

[23] L. Wang, "Numerical simulation and analysis of carbon-reinforced rubber's Mullins effect," *Chinese Journal of Computational Mechanic*, vol. 34, no. 3, pp. 372–378, 2017 (Chinese).